Continuum limit in random sequential adsorption

V. Privman,* J.-S. Wang, and P. Nielaba
Institut für Physik, Johannes-Gutenberg-Universität Mainz, Staudinger Weg 7, D-6500 Mainz, Federal Republic of Germany
(Received 9 August 1990)

We develop analytical estimates of the late-stage (long-time) asymptotic behavior of the coverage in the D-dimensional lattice models of irreversible deposition of hypercube-shaped particles. Our results elucidate the crossover from the exponential time dependence for the lattice case to the power-law behavior with a multiplicative logarithmic factor, in the continuum deposition. Numerical Monte Carlo results are reported for the two-dimensional (2D) deposition, both lattice and continuum. Combined with the exact 1D results, they are used to test the general theoretical expectations for the late-stage deposition kinetics. New accurate estimates of the jamming coverages in 2D rule out some earlier "exact" conjectures. Generally, a combination of lattice and continuum simulations, with asymptotic crossover analysis, allows for a deeper understanding of the deposition kinetics and derivation of improved numerical estimates.

I. INTRODUCTION

In many experiments on adhesion of colloidal particles and proteins on substrates, the relaxation time scales are much longer than the times of the formation of the deposit.[1-5] Much theoretical attention has been devoted to the problem of *irreversible monolayer* particle deposition termed random sequential adsorption (RSA) or the car-parking problem.[6-25] A quantity of central interest is the fraction of the total volume [area in two dimensions (2D)] covered by the depositing particles $\theta(t)$. Because of the blocking effect by the already deposited particles of the volume (area) available for deposition of additional particles, the limiting value $\theta(\infty)$ is less than the close packing. The formation of the limiting jammed state is governed by the infinite memory correlation effects, due to the absence of relaxation. Therefore, the time dependence of $\theta(t)$ cannot be described by the mean-field theory except for very short times[23] for which $\theta(t) \propto t$.

Theoretical studies[6-25] of the RSA processes invoked various methods ranging from series expansions to numerical Monte Carlo simulations. Exact results are available in 1D (see, e.g., Ref. 9). For continuum deposition models, the long-time behavior is generally given by the power law,

$$\theta(t)=\theta(\infty)-\frac{\text{const}(\ln t)^q}{t^p} , \tag{1.1}$$

where $q=0$ in most cases. In 1D one has $p=1$, $q=0$ (see Ref. 9). Analytical arguments[11,12] support the numerical conjecture[10] that $p=1/D$ (and $q=0$) for deposition of spherical objects in D dimensions. However, there are analytical[12] and numerical[20,22] indications that the precise form of the convergence law depends on the shape and orientational freedom of the depositing objects.

Numerical simulations of continuum deposition are exceedingly difficult, and even the results of very long Monte Carlo runs are difficult to interpret unambiguously.[20,22] On the other hand, lattice model simulations are easier to perform.[16-18,24] However, the approach to the jamming coverage is asymptotically exponential in lattice deposition models:

$$\theta(t)=\theta(\infty)-\text{const}\, e^{-t/\sigma} . \tag{1.2}$$

In the present work we consider the deposition of fixed-orientation squares on 2D substrates. For the continuum version of the deposition of hypercubic objects of fixed orientation in D dimensions, Swendsen[12] proposed an analytical argument for the asymptotic law (1.1) with $q=D-1$ and $p=1$. The purpose of our study is to develop an analytical theory elucidating the crossover from the characteristic lattice behavior (1.2) to the continuum asymptotic form and to test various phenomenological predictions by lattice and continuum Monte Carlo simulations in 2D.

Generally, the crossover from the lattice to continuum behavior in irreversible kinetics has not been investigated in the literature, except for the exact results for the deposition of k-mers in 1D, which can be analyzed in the limit $k \to \infty$ (see Ref. 9). Our analytical considerations, presented in Secs. II and III, generalize the "continuum" ideas of Refs. 11 and 12 to the lattice kinetics. Predictions of the phenomenological theory are compared, in Sec. IV, with the asymptotic expressions derivable from the exact solution[9] of the deposition of k-mers on lattices in 1D. The Monte Carlo simulation of the 2D deposition of oriented squares is described in Sec. V. The results for the jamming coverages are given in Sec. VI. Sections VII and VIII are devoted, respectively, to the comparison of the Monte Carlo results with the phenomenological long-time asymptotic predictions and with the continuum-limit behavior. Finally, Sec. IX gives a brief summary and discussion.

II. LONG-TIME RSA KINETICS: FROM LATTICE TO CONTINUUM

We consider the deposition of (hyper)cubic objects of fixed orientation and of size l^D on a D-dimensional substrate. Let us assume that the substrate has dimensions L^D and cubic shape aligned with the orientation of the depositing l^D cubes. It is also convenient to visualize L as an integral multiple of l. However, we will always assume $L \to \infty$ an an implicit limit taken before any other limits, so that we do not concern ourselves with finite-size effects. The rate of random deposition attempts will be denoted by R and measured per unit time and volume. A point in the volume L^D is chosen at random, with a uniform probability density. It marks the location of a hypercube of size l^D, e.g., by being the cube's center. If this cube does not overlap any other cubes already in place, it is "deposited." Otherwise, the attempt is discarded.

The lattice approximation is introduced by choosing the cubic mesh size $b=l/k$. A hypercubic lattice of spacing b is fixed parallel to the axes of the total volume L^D. The lattice deposition is defined by requiring that the objects of size l^D can only deposit in sites consisting of k^D lattice unit cubes, and the depositing cubes must coincide exactly with their lattice subcubes. Thus the deposition is no longer continuous, but is discretized and occurs only in $(L/b)^D$ sites (we neglect boundary effects). In order to preserve the overall deposition rate, the deposition attempt rate at each allowed lattice location (site) must be Rb^D (per unit time).

According to Refs. 11 and 12, the late stage of the deposition in continuum can be described as the filling up of voids small enough to accommodate only one depositing object. The deposition process consists of two types of events. Large gaps are partially filled by the depositing objects leaving smaller gaps. Gaps small enough so that only one object can fit in are also filled up, simultaneously with the first process. However, there should exist a certain time τ after which most of the large gaps have been eliminated and the deposition process is dominated by the small gaps. At this time τ, the density of those small gaps (number of gaps per unit volume) will be ρ, and one can further assume[11,12] that gaps of various shapes have roughly equal density.

For lattice models a similar picture should apply for sufficiently large k values. The correct condition turns out to be $k^D \gg Rl^D\tau$. Specifically, for the deposition of (hyper)cubes, typical small gaps can be assumed[12] to have rectangular shapes, with edges along the lattice directions. For counting purposes, we can classify these "small voids" as rectangular boxes (or close, near-rectangular shapes) of sizes $[(k+n_1)\times(k+n_2)\times\cdots\times(k+n_D)]$, measured in lattice spacings. The integers n_j can take on values $n_j=0,1,\ldots,k-1$, in order to prevent deposition of more than one object in a void. In this approximate classification of the gaps, there are k^D different types of gaps. Each type will have density ρ/k^D at time τ and will be filled up at the rate $[Rb^D(n_1+1)(n_2+1)\cdots(n_D+1)]$ per unit time. We will consider the regime of $t \gg \tau$ so that no new small gaps are created by the filling up of large gaps. Then the density Ω of each type of small gap ("type" being specified by the set n_j) will have the following time dependence:

$$\Omega(n_j)=\frac{\rho}{k^D}e^{-Rb^D(n_1+1)\cdots(n_D+1)(t-\tau)} . \tag{2.1}$$

We now recall that the coverage θ is defined as the fraction of the volume covered by cubes. In each deposition event it is increased by $(l/L)^D$. The rate of such events per unit time, for each type of gap, is just $[Rb^D\Omega(n_j)\prod_{m=1}^{D}(n_m+1)]$. Thus we have

$$\frac{d\theta}{dt}\simeq\sum_{n_1=0}^{k-1}\cdots\sum_{n_D=0}^{k-1}\frac{Rb^Dl^D\rho}{k^D}\left[\prod_{j=1}^{D}(n_j+1)\right]\exp\left[-Rb^D\left[\prod_{m=1}^{D}(n_m+1)\right](t-\tau)\right] . \tag{2.2}$$

This relation can be integrated to yield the asymptotic ($t \gg \tau$) estimate

$$\theta_k(t)=\theta_k(\infty)-\frac{\rho l^D}{k^D}\sum_{n_1=0}^{k-1}\cdots\sum_{n_D=0}^{k-1}\exp\left[-\left[\frac{Rl^D}{k^D}\right]\left[\prod_{m=1}^{D}(n_m+1)\right](t-\tau)\right] , \tag{2.3}$$

where the k dependence of $\theta_k(\infty)$ for $k^D \gg Rl^D\tau$ should be smooth and have no interesting features. We will omit the k dependence of $\theta_k(t)$ in most of the expressions below.

We further note that the expressions (2.2) and (2.3) can only be used as the leading-order estimates. Indeed, the limits of large k and t have been assumed, and at the present level of the derivation we have no control of the corrections. Thus we can modify these relations as long as the *leading* behavior is preserved. The most important such change is to replace $(t-\tau)$ by t, thus neglecting terms of relative magnitude $Rl^D\tau/k^D$, as compared to the leading-order t-dependent terms. This suggests that (2.2) and (2.3) provide in fact a *one-parameter* ρ asymptotic representation of the coverage. The result is also quite insensitive to the upper limits in the sums over n_j, but the present form is as convenient as other choices. Thus we replace (2.3) by

$$\theta_k(t)=\theta_k(\infty)-\frac{\rho l^D}{k^D}\sum_{n_1=0}^{k-1}\cdots\sum_{n_D=0}^{k-1}\exp\left[-\left[\frac{Rl^Dt}{k^D}\right]\prod_{m=1}^{D}(n_m+1)\right] . \tag{2.4}$$

III. LONG-TIME RSA KINETICS: SPECIAL LIMITS

In this section we consider some special limits in which relation (2.4) is reducible to less cumbersome forms. First, for k fixed, the "lattice" long-time behavior sets in for $Rl^D t \gg k^D$. In this limit the $n_j=0$ term in the sums in (2.4) dominates:

$$\theta(t)\approx\theta(\infty)-\frac{\rho l^D}{k^D}e^{-Rl^D t/k^D} . \tag{3.1}$$

Thus the time decay constant in Eq. (1.2) increases as k^D:

$$\sigma\approx k^D/(Rl^D) \quad (k \text{ large}) . \tag{3.2}$$

The continuum limit of (2.4) is obtained for $k^D \gg Rl^D t$. In this limit one can convert the sums to integrals:

$$\theta(t)\approx\theta(\infty)-\rho l^D\int_0^1 dx_1\cdots\int_0^1 dx_D \exp(-Rl^D t x_1 x_2\cdots x_D) . \tag{3.3}$$

Recall that all the expressions here apply only for $t\gg\tau$ and $k^D\gg Rl^D\tau$, where $Rl^D\tau$ is a fixed quantity of order 1. Thus the large-k and large-t conditions are simply $k\gg 1$ and $t\gg(Rl^D)^{-1}$. The latter condition allows us to evaluate the integrals in (3.3) asymptotically, to the leading order for large t, which yields

$$\theta(t)\approx\theta(\infty)-\frac{\rho[\ln(Rl^D t)]^{D-1}}{(D-1)!Rt} . \tag{3.4}$$

The asymptotic $(\ln t)^{D-1}/t$ law was derived in Ref. 12 for the continuum deposition of cubic objects.

IV. EXACT 1D RESULTS AND SCALING INTERPRETATION

In 1D it is convenient to consider the derivative expression (2.2) in which we replace τ by 0 (see Sec. II), and we further extend the summation to ∞, which amounts to neglecting a contribution of order $\exp(-Rlt)$. Furthermore, let us introduce the dimensionless time variable

$$T\equiv Rl^D t . \tag{4.1}$$

The 1D version of (2.2) then yields

$$\frac{d\theta}{dT}\simeq\frac{\rho l e^{-T/k}}{k^2(1-e^{-T/k})^2} . \tag{4.2}$$

The exact solution is given by[9]

$$\theta=\int_0^{k(1-e^{-T/k})}du\,\exp\left\{-2\int_0^u v^{-1}\left[1-\left[1-\frac{v}{k}\right]^{k-1}\right]dv\right\} , \tag{4.3}$$

which yields

$$\frac{d\theta}{dT}=\exp\left\{-\frac{T}{k}-2\int_0^{k(1-e^{-T/k})}v^{-1}\left[1-\left[1-\frac{v}{k}\right]^{k-1}\right]dv\right\} . \tag{4.4}$$

Both our asymptotic considerations and the exact 1D solution suggest the *scaling-limit interpretation:* Let $k\to\infty$ and $T\to\infty$ with the fixed ratio T/k^D. As long as T/k^D ($D=1$) is a finite positive constant, the large-k limit of (4.4) can be calculated as follows. First replace

$$\left[1-\frac{v}{k}\right]^{k-1}\simeq e^{-v} . \tag{4.5}$$

Then note that for large positive X, we have

$$\int_0^X\frac{1-e^{-v}}{v}dv\simeq\gamma+\ln X , \tag{4.6}$$

where $\gamma=0.577\,215\,664\,9\ldots$ is the Euler's constant. These relations, with

$$X\equiv k(1-e^{-T/k}) , \tag{4.7}$$

reduce the exact result (4.4) to the asymptotic expression (4.2), provided we identify

$$\rho l\equiv e^{-2\gamma} \quad (D=1) . \tag{4.8}$$

Thus the asymptotic estimate (4.2) applies in the scaling limit. In the two extremes $T\gg k$ and $T\ll k$, we expect (3.1) and (3.4) to hold. While the $T\ll k$ case is straightforward, the above derivation must be considered with caution in the case $T\gg k$ because the upper limit in the v integration is close to k and (4.5) cannot be used. However, we checked by a different limiting procedure not detailed here that (3.1) is indeed obtained from the exact solution. (Recall that for general D, the limiting regimes are defined by $T\gg k^D$ and $T\ll k^D$.)

The analysis of the k dependence of $\theta_k(t=\infty)$ is mathematically complicated, and it was not attempted

here. Numerical results for several k, up to $k=1000$, were reported and discussed in Ref. 9.

We also compared the predictions (3.1) and (4.2) with the results of a numerical integration of the exact expression for the time-dependent coverage in $D=1$. For times $T>10k$ the approximants calculated according to (3.1) and (4.2) agree with the exact results within 10^{-6} for different values of k ($k=2,10,100$), and the differences decrease exponentially in time for longer times. For shorter times ($T\lesssim 10k$) the full asymptotic form (4.2) gives better agreement with the exact results than (3.1).

V. MONTE CARLO ALGORITHMS FOR 2D DEPOSITION

The RSA model of the 2D deposition was studied by computer simulations on a periodic $(N\times N)$ lattice of unit spacing. Initially, the lattice site occupancy variables $I(x,y)$ were set to the *empty* values $I(x,y)=0$. At each deposition attempt, a site (x_0,y_0) was chosen at random. If $I(x,y)=0$ for $x_0\le x<x_0+k$ and $y_0\le y<y_0+k$, then a $(k\times k)$-mer was put on the lattice: We set $I(x,y)=1$ at these k^2 sites; otherwise, the attempt was rejected. The Monte Carlo time variable was defined in such a way that a unit time step consisted of exactly $(N/k)^2$ deposition attempts. One can check that this definition corresponds to the dimensionless time variable T defined in (4.1), and it differs from that used in Ref. 24 by a factor k^2.

Three different updating schemes were used in our calculations.

Algorithm 1: A direct implementation of the steps described above; $I(x,y)$ is stored as an integer (or logical) array $(N\times N)$. This algorithm is efficient for smaller k. However, it becomes inefficient for larger k values because the computer time per one trial increases as k^2, while the memory requirements grow as N^2. Thus it was used only for $k=2,3$ and for testing the other methods.

Algorithm 2: The system is divided into square boxes of size $(k\times k)$; recall that we always take N as an integral multiple of k. For each deposition attempt at (x_0,y_0) as described earlier, one checks the box containing (x_0,y_0) and eight boxes around it for overlap. The coordinates of the $(k\times k)$-mers deposited can be stored in an array of size $(N/k)\times(N/k)$. The computer time (per attempt) is constant with k. In fact, a continuum deposition was also simulated by using this bookkeeping method, with $k=1$ and (x,y) allowed to assume real-number values. For the discrete deposition, memory requirements are reduced by a factor k^{-2} as compared to algorithm 1. Most of our time-dependence data were obtained by using algorithm 2.

Algorithm 3: For late times $T\gg k^2$, most of the attempts are rejected. The acceptance rate is exponentially small, $\sim e^{-T/k^2}$ [see (3.1)]. A more efficient way for calculations near the jamming limit was devised based on this observation. We used the same data structures as in algorithm 2. In addition, an auxiliary list was employed to store all the possible sites for further deposition after the initial Monte Carlo run for $T\lesssim k^2$. For $T\gtrsim k^2$ we chose sites at random only from this list, which was in turn updated after a certain number of attempts. The jamming limit was reached when the auxiliary list was exhausted. The time-dependence information could be obtained with a suitable renormalization of time by the inverse of the fraction of the "available" deposition sites. However, we only used algorithm 3 for the determination of the jamming coverages (Sec. VI).

VI. JAMMING COVERAGES IN 2D

The maximum coverage (jamming coverage) values have been investigated by several authors (see Refs. 13, 16, and 18, and literature quoted therein). We used algorithm 3 for estimating $\theta_k(\infty)$, as described in Sec. V. The results are summarized in Table I. These data were obtained for system sizes $N/k=200$. For such sizes the finite-size effects can be neglected when compared with the statistical spread of the resulting estimates. Indeed, for $k=2$, for instance, we checked that the differences in the jamming coverages obtained with $N/k=10$, 200, and 500 are comparable with statistical errors. Recall that we used periodic boundary conditions which tend to yield the smallest finite-size effects quite generally. In 2D simulations finite-size corrections of order k/N are expected for free (open) boundary conditions.[16]

When plotted versus $1/k$, the $\theta_k(\infty)$ estimates show a slight curvature, which suggests a fit to the form

$$\theta_k(\infty)=\theta_\infty(\infty)+\frac{A_1}{k}+\frac{A_2}{k^2}+\cdots . \tag{6.1}$$

By the standard manipulations of the sequence given in Table I to cancel the leading $1/k$ term, followed by a further extrapolation to $k\to\infty$ (see Ref. 26 for a review), we arrived at the estimate

$$\theta_\infty(\infty)=0.5620\pm 0.0002 . \tag{6.2}$$

Our jamming coverage estimates are generally consistent with and more accurate than the previous results.[13,16,18] The errors are small enough to rule out the conjecture of Palásti,[27] and its generalization for finite k,[28] which state that the jamming coverages for the 2D $(k\times k)$ oriented squares are equal to the *squared* jamming coverages of the corresponding 1D k-mer models. The latter are known exactly.[9] Our numerical ranges are

TABLE I. Jamming coverage estimates for the 2D lattice deposition of $(k\times k)$ oriented squares. The error bars shown are statistical. The data were averaged over several Monte Carlo runs, the number of which is given.

k	$\theta_k(\infty)$	Runs
2	0.747 93±0.000 01	30 000
3	0.679 61±0.000 01	30 000
4	0.647 93±0.000 01	15 000
5	0.629 68±0.000 01	17 000
10	0.594 76±0.000 04	4 400
20	0.578 07±0.000 05	600
50	0.568 41±0.000 10	150
100	0.565 16±0.000 10	199

quite close to the conjectured values (but do not include them). For a given k the differences are about half a percent of the $\theta_k(\infty)$ value. To check for the possibility that the difference might be due to a subtle correlation of the random numbers in the longest runs which are those that yield the jamming coverages, we used three different random-number generators: VAX-Fortran supplied random numbers, exclusive-OR algorithm (R250), and a hybrid of R250 and a simple linear-congruent random-number generator. All runs gave the same results.

VII. MONTE CARLO RESULTS (2D) FOR LONG AND INTERMEDIATE TIMES

In this section we describe the coverage data $\theta_k(T)$ obtained by Monte Carlo simulations for $k=2$, 3, 5, 10, and 20, for times $T \leq 1000$. These data were obtained by implementing algorithms 1 and 2, on lattices of sizes $N=200k$. For $k \leq 10$ the T values up to 1000 are large enough to see clearly the exponential decay [see (3.1)]. Let us rewrite (3.1) as

$$k^2[\theta_k(\infty)-\theta_k(T)]=\rho l^2 e^{-\Sigma T/k^2} \quad (D=2) . \tag{7.1}$$

Then the theoretical prediction (3.2) is $\Sigma \equiv 1$.

Our data are shown in Fig. 1. It appears that a clear straight-line behavior on a semilogarithmic plot of $[\theta(\infty)-\theta(T)]$ versus T is obtained for times $T \gtrsim 3k^2$. The slopes of the asymptotic straight lines for $k \leq 10$ suggest the Σ estimates 1.002, 0.984, 0.977, and 1.095, for $k=2$, 3, 5, and 10, respectively. It is difficult to assign reliable error bars to these numbers. However, these estimates confirm the theoretical value $\Sigma \equiv 1$.

The dimensionless amplitude ρl^2 in (7.1) follows from the intercepts of the straight-line fits. The data of Fig. 1 yield the values

$$\rho l^2 \simeq 0.490,\ 0.424,\ 0.414,\ \text{and}\ 0.663 , \tag{7.2}$$

for $k=2$, 3, 5, and 10, respectively. Here again it is difficult to decide what are the error limits.

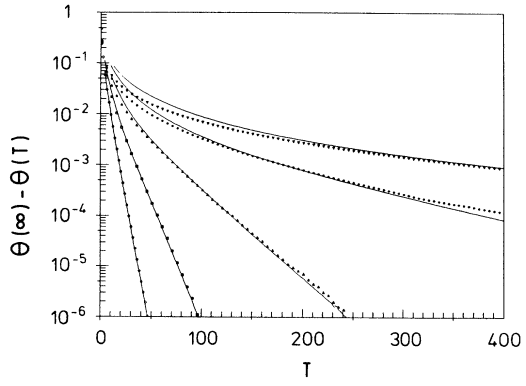

FIG. 1. Time dependence of the coverage in the 2D lattice deposition of squares of sizes $k=2$, 3, 5, 10, and 20. The top-most data are $k=20$, and the lower data sets correspond to the decreasing k values. The solid curves correspond to the asymptotic expression (2.4), with $\rho=0.44l^{-2}$.

The phenomenological prediction (2.4) involves only one parameter ρ. Thus, in Fig. 1, we plotted the functions (2.4) for each k value, taking $\rho l^2=0.44$ in all five cases. The solid curves (Fig. 1) thus obtained indeed follow the numerical data and in fact provide a quantitatively good representation especially for the smaller-k data. Recall that (2.4) is the leading-order asymptotic prediction, and in fact it should apply for large enough k and T. The fact that "large k" is actually quite small is an empirical observation. The uncertainty in the ρ values and the difficulty in obtaining high-quality numerical data for larger-k values in the regime $T \geq k^2$ preclude a detailed check of (2.4) for $k > 20$.

It is in fact possible that (2.4) sometimes applies for rather small-k values. Indeed, the only aspect of the derivation of (2.4) that seems to require large k is the assumption that the densities of voids of various shapes are roughly equal at the time τ. For large k we can assume this property for a nearly continuous void-shape distribution based on the success of the "continuum-deposition" arguments of Refs. 11 and 12, which were checked by several numerical and analytical studies for a range of deposition problems. For small k, when only a few void shapes are possible, the equal-density assumption may well break down. In fact, we did use $k \gg 1$ in (4.5), in the 1D case.

VIII. RESULTS FOR THE 2D DEPOSITION IN THE CONTINUUM LIMIT

In this section we describe the analysis of the coverage data obtained for $k=2$, 3, 5, 10, 20, 50, and ∞ (a direct continuum simulation described in Sec. V, with algorithm 2). As before, these data were obtained by implementing algorithms 1 and 2, on lattices of sizes $N=200k$, with the longest runs up to $T=1000$. However, the focus of this section is on the continuum limit which according to the phenomenological expectations is reached in the regime $k^2 \gg T$.

In Fig. 2, $[\theta_k(\infty)-\theta_k(T)]$ estimates are plotted on a double logarithmic scale. It is clear that the data for

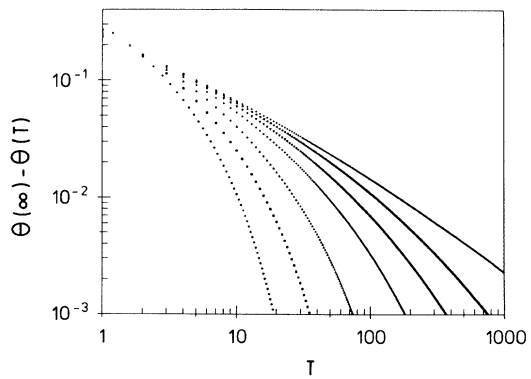

FIG. 2. Monte Carlo data as in Fig. 1, supplemented by the $k=\infty$ results (top-most set) and the $k=50$ results (second set from the top), plotted on a double logarithmic scale. The lower data sets are for $k=20$, 10, 5, 3, and 2.

finite k break off the $k=\infty$ results for T values which are considerably less than k^2. The present k values are not large enough to decide unambiguously if the criterion $T/k^2=O(1)$ is replaced by another proportionality law, e.g., $T\sim k^\kappa$, with $\kappa<2$, or if one has a proportionality constant in $T\sim k^2$ much less than 1. In any case this crossover feature of our Monte Carlo results is not described correctly by the phenomenological theory.

Because of the presumably logarithmic correction [see (3.4)], the slope of the curves in Fig. 2 continuously varies with T. We tried several fits of the data for $[\theta_\infty(\infty)-\theta_\infty(T)]$ to a simple power law (without logarithms). The effective exponent $p_{\rm eff}$ thus obtained shows a slow but clear convergence to the expected value $p=1$ [see (1.1) and (3.4)]. Note that we used the central value of (6.2) for $\theta_\infty(\infty)$. Indeed, for this quantity the lattice extrapolation as described in Sec. VI was found to yield more accurate results than the direct extrapolation of the numerical estimates of $\theta_\infty(T)$ to the $T\to\infty$ limit.

The available data are not sufficient to obtain reliable estimates of both powers p and q in (1.1). As a further evidence supporting (3.4), let us impose $p=1$ and test the logarithmic time dependence of $T[\theta_\infty(\infty)-\theta_\infty(T)]$. The data for this quantity versus T is shown in Fig. 3. A linear relation is clearly seen for $T\gtrsim 50$. The data for $50\le T\le 800$ can be fitted well by

$$T[\theta_\infty(\infty)-\theta_\infty(T)]\simeq(\rho l^2)\ln T+c\ , \tag{8.1}$$

with $(\rho l^2)=0.379$ and $c=-0.296$. The data for $T>800$ were excluded because of the statistical noise (see Fig. 3). The ρl^2 value is roughly consistent with the estimates given in (7.2), based on the analysis in the regime $T\gg k^2$. The uncertainties in ρl^2 estimates in both asymptotic regimes are large and difficult to estimate reliably.

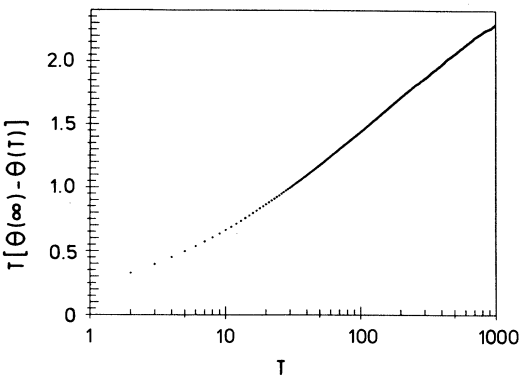

FIG. 3. Monte Carlo results for $T[\theta_\infty(\infty)-\theta_\infty(T)]$, calculated with the central estimated value (6.2), $\theta_\infty(\infty)=0.5620$.

IX. SUMMARY AND DISCUSSION

In this work we developed a phenomenological theory of the late-stage deposition of fixed-orientation hypercubes, with emphasis on the lattice deposition and crossover to the continuum limit. Our main analytical result is (2.4) and its asymptotic limits (3.1) and (3.4). Exact 1D calculations confirm the phenomenological theory.

Monte Carlo algorithms for studying the 2D deposition were developed and applied both for the lattice and continuum cases. The 2D data confirm the theory in most of their features. The observed discrepancy (Sec. VIII) with the crossover criterion $T\sim k^2$ calls for further study and elucidation.

Our numerical results provide new high-accuracy jamming coverage estimates in 2D and rule out the conjecture relations[27,28] to the squared 1D jamming values.

Note added in proof. Recently, new numerical results were reported[29] for the continuum deposition of squares, providing an accurate verification of the $(\ln t/t)$ asymptotic behavior of $[\theta_\infty(\infty)-\theta_\infty(t)]$. This new study[29] also yielded the improved jamming coverage estimate $\theta_\infty(\infty)=0.562\,009\pm0.000\,004$, as well as $\theta_k(\infty)$ values for $k=2, 4, 8, 16, 32, \ldots$. These results are consistent with our estimates for $k=2, 4, \infty$, see (6.2) and Table I.

ACKNOWLEDGMENTS

The authors wish to thank Professor Kurt Binder for helpful discussions and to acknowledge the financial assistance of the Sonderforschungsbereich 262 of the Deutsche Forshungsgemeinschaft.

*Permanent address: Department of Physics, Clarkson University, Potsdam, NY 13699-5820.

[1]J. Feder and I. Giaever, J. Colloid Interface Sci. **78**, 144 (1980).
[2]A. Schmitt, R. Varoqui, S. Uniyal, J. L. Brash, and C. Pusiner, J. Colloid Interface Sci. **92**, 25 (1983).
[3]G. Y. Onoda and E. G. Liniger, Phys. Rev. A **33**, 715 (1986).
[4]N. Kallay, M. Tomić, B. Biškup, I. Kunjašić, and E. Matijević, Colloids Surf. **28**, 185 (1987).
[5]J. D. Aptel, J. C. Voegel, and A. Schmitt, Colloids Surf. **29**, 359 (1988).
[6]P. J. Flory, J. Am. Chem. Soc. **61**, 1518 (1939).
[7]A. Rényi, Publ. Math. Inst. Hung. Acad. Sci. **3**, 109 (1958).
[8]B. Widom, J. Chem. Phys. **44**, 3888 (1966).
[9]J. J. Gonzalez, P. C. Hemmer, and J. S. Høye, Chem. Phys. **3**, 228 (1974). The kinetics of the dimer ($k=2$) deposition in 1D was solved earlier, see E. R. Cohen and H. Reiss, J. Chem. Phys. **38**, 680 (1963).
[10]J. Feder, J. Theor. Biol. **87**, 237 (1980).
[11]Y. Pomeau, J. Phys. A **13**, L193 (1980).
[12]R. H. Swendsen, Phys. Rev. A **24**, 504 (1981).
[13]R. S. Nord and J. W. Evans, J. Chem. Phys. **82**, 2795 (1985).
[14]J. W. Evans and R. S. Nord, J. Stat. Phys. **38**, 681 (1985).
[15]L. A. Rosen, N. A. Seaton, and E. D. Glandt, J. Chem. Phys. **85**, 7359 (1986).
[16]M. Nakamura, J. Phys. A **19**, 2345 (1986).
[17]M. Nakamura, Phys. Rev. A **36**, 2384 (1987).
[18]G. C. Barker and M. J. Grimson, Mol. Phys. **63**, 145 (1988).
[19]P. Schaaf, J. Talbot, H. M. Rabeony, and H. Reiss, J. Phys. Chem. **92**, 4826 (1988).
[20]R. D. Vigil and R. M. Ziff, J. Chem. Phys. **91**, 2599 (1989).

[21]P. Schaaf and J. Talbot, Phys. Rev. Lett. **62**, 175 (1989).
[22]J. Talbot, G. Tarjus, and P. Schaaf, Phys. Rev. A **40**, 4808 (1989).
[23]M. C. Bartelt and V. Privman, J. Chem. Phys. **93**, 6820 (1990).
[24]P. Nielaba, V. Privman, and J.-S. Wang, J. Phys. A (to be published).
[25]R. Dickman (private communication).
[26]A. J. Guttmann, in *Phase Transitions and Critical Phenomena,* edited by C. Domb and J. L. Lebowitz (Academic, New York, 1989), Vol. 13, p. 1.
[27]I. Palásti, Publ. Math. Inst. Hung. Acad. Sci. **5**, 353 (1960).
[28]E. M. Tory, W. S. Jodrey, and D. K. Pickard, J. Theor. Biol. **102**, 439 (1983).
[29]B. J. Brosilow, R. M. Ziff, and R. D. Vigil, Phys. Rev. A (to be published).